

# Entanglement and Optimal Timing in Discriminating Quantum Dynamical Processes

Massimiliano F Sacchi<sup>1,2</sup>

<sup>1</sup> CNR - Istituto di Fotonica e Nanotecnologie, Piazza Leonardo da Vinci 32, I-20133, Milano, Italy

<sup>2</sup> QUIT Group, Dipartimento di Fisica, Università degli Studi di Pavia, Via Agostino Bassi 6, I-27100 Pavia, Italy

**Abstract.** I investigate the problem of optimally discriminating between two open quantum dynamical processes in a single-shot scenario, with the goal of minimizing the error probability of identification. This task involves optimising both the input state—potentially entangled with an ancillary system that remains isolated from the dynamics—and the time at which the resulting time-dependent quantum channels, induced by the two distinct dynamical maps, becomes most distinguishable. To illustrate the complexity and richness of this problem, I focus on Pauli dynamical maps and their associated families of time-dependent Pauli channels. I identify a regime in which separable strategies require waiting indefinitely for the dynamics to reach the stationary state, whereas entangled input states enable optimal discrimination at a finite time, with a strict reduction in error probability. These results highlight the crucial interplay between entanglement and timing in enhancing the distinguishability of quantum dynamical processes.

*Keywords:* Quantum dynamical processes; entanglement and optimal timing; optimal discrimination

## 1. Introduction

Discriminating among alternative hypotheses is a fundamental task in both foundational and applied aspects of quantum information theory. The most prominent example is the problem of minimizing the error probability in quantum state discrimination, originally formulated by Helstrom [1]. This challenge has since been extensively explored in a variety of settings [2–11], including the discrimination of unitary transformations [12–14] and general quantum channels [15–19]. In particular, for minimum-error discrimination between two quantum channels, it is well established that the use of entangled input states can offer a strict advantage—even in highly noisy scenarios, such as when dealing with entanglement-breaking channels [16]. This key insight has led to the development of quantum illumination protocols [20–23], where entangled states of light enhance the detection of weak signals embedded in noisy environments.

In this work, I focus on the problem of distinguishing between two known open quantum dynamical processes, aiming to minimize the error probability in a single-shot setting. I formulate the problem as jointly optimising both the input state—which may be entangled with an ancillary system that remains isolated from the dynamics—and the time at which the time-dependent quantum channels, generated by the two distinct processes, are most distinguishable. The analysis presented here highlights the deep connection between entanglement, temporal dynamics, and optimal discrimination, offering new insights into the role of quantum resources in hypothesis testing.

To illustrate the complexity of the problem and the diversity of its solutions, I present a detailed analysis of Pauli dynamical maps and their corresponding families of time-dependent Pauli channels. These channels model relevant noise processes in qubit systems and serve as an instructive testbed for exploring optimal discrimination strategies [24, 25]. I show that in certain cases, optimal discrimination without entanglement requires an indefinitely long waiting time—until the process reaches its stationary state. In contrast, the use of entangled input states enables discrimination at a finite optimal time, along with a significant reduction in the error probability. These findings underscore the crucial role of entanglement and precise timing in enhancing the distinguishability of quantum dynamical processes.

Finally, I note that prior studies using quantum probes to discriminate between thermal baths, characterized by different temperatures [26, 27] or statistical properties [28, 29], can be viewed as specific instances of the general problem of distinguishing open quantum dynamics.

## 2. Discriminating quantum dynamical processes

A quantum dynamical process is governed by a generator  $\mathcal{L}_t$  which dictates the evolution of the system density matrix  $\rho(t)$  through the differential equation  $\partial_t \rho(t) = \mathcal{L}_t \rho(t)$ . Under suitable physical conditions, the generator  $\mathcal{L}_t$  can assume particularly tractable forms as, for example,  $\mathcal{L}_t = -i[H_t, \cdot]$  for Hamiltonian dynamics, or a GKSL-like form for

Markovian divisible evolution [30,31]. Anyway, to represent a physically valid evolution, at any time  $t$  the associated map  $\mathcal{E}_t = \mathcal{T} \exp(\int_0^t \mathcal{L}_s ds)$ , defined via the time-ordered exponential of  $\mathcal{L}_t$ , must be a quantum channel—i.e. a trace-preserving completely positive map [30, 31]. In fact, this map  $\mathcal{E}_t$  provides the quantum state  $\rho(t)$  at time  $t$  from the initial state  $\rho(0)$  as  $\rho(t) = \mathcal{E}_t(\rho(0))$ .

Now consider a scenario in which the evolution of a quantum system is known to be governed by one of two candidate dynamical processes, generated by  $\mathcal{L}_t^{(1)}$  and  $\mathcal{L}_t^{(2)}$ , occurring with prior probabilities  $q_1$  and  $q_2 = 1 - q_1$ , respectively. The problem of distinguishing between these two dynamics reduces to identifying the optimal time  $t^*$  at which a discrimination test between the corresponding time-dependent quantum channels  $\mathcal{E}_t^{(1)}$  and  $\mathcal{E}_t^{(2)}$  minimises the probability of error. This optimisation may include the use of entangled input states to enhance distinguishability.

To frame this problem, I briefly recall the main results from Ref. [15] on minimum-error discrimination between two generic quantum channels  $\mathcal{E}^{(1)}$  and  $\mathcal{E}^{(2)}$ , given with prior probabilities  $q_1$  and  $q_2$ . This problem is formulated by seeking the optimal input state  $\rho$  on the Hilbert space  $\mathcal{H}$  such that the error probability in discriminating the corresponding output states  $\mathcal{E}^{(1)}(\rho)$  and  $\mathcal{E}^{(2)}(\rho)$  is minimised. If side entanglement is allowed, the output states to be distinguished take the form  $(\mathcal{E}^{(1)} \otimes \mathcal{I})\rho$  and  $(\mathcal{E}^{(2)} \otimes \mathcal{I})\rho$ , where the input  $\rho$  is generally a bipartite state on  $\mathcal{H} \otimes \mathcal{K}$ , and the quantum channels act solely just on the first subsystem, while the trivial identity map  $\mathcal{I}$  acts on the second. Notably, the use of entanglement can strictly enhance discrimination, even in highly noisy scenarios [16].

The foundational result by Helstrom [1] states that the minimum error probability  $p'_E$  in optimally discriminating between two quantum states  $\rho_1$  and  $\rho_2$ , given with prior probabilities  $q_1$  and  $q_2$ , is given by

$$p'_E = (1 - \|q_1\rho_1 - q_2\rho_2\|_1)/2, \quad (1)$$

where  $\|A\|_1 = \text{Tr}\sqrt{A^\dagger A}$  denotes the trace norm of  $A$ . This result inherently accounts for the corresponding optimal (binary and orthogonal) measurement.

Then, for quantum channel discrimination with no use of entanglement, the minimum error probability  $\tilde{p}_E$  is given by

$$\tilde{p}_E = (1 - \max_{\rho} \|q_1\mathcal{E}^{(1)}(\rho) - q_2\mathcal{E}^{(2)}(\rho)\|_1)/2, \quad (2)$$

where  $\rho$  ranges over all density matrices on  $\mathcal{H}$ . On the other hand, when entangled input states are allowed, the minimum error probability  $p_E$  is given by

$$p_E = (1 - \max_{\rho} \|q_1(\mathcal{E}^{(1)} \otimes \mathcal{I})\rho - q_2(\mathcal{E}^{(2)} \otimes \mathcal{I})\rho\|_1)/2, \quad (3)$$

where now  $\rho$  is a density matrix on  $\mathcal{H} \otimes \mathcal{K}$ . The maximum of the trace norm in Eq. (3) is known as the norm of complete boundedness (or diamond norm). In fact, for finite-dimensional Hilbert space, one can simply take  $\mathcal{K} = \mathcal{H}$  [32, 33]. Moreover, due to the convexity of the trace norm, in both Eqs. (2) and (3) the maximum can be searched for among pure states.

It follows that the error probabilities in discriminating between the two dynamical maps  $\mathcal{L}_t^{(1)}$  and  $\mathcal{L}_t^{(2)}$  at time  $t$  can be obtained from Eqs. (2) and (3) by replacing  $\mathcal{E}^{(i)}$  with  $\mathcal{E}_t^{(i)} = \mathcal{T} \exp(\int_0^t \mathcal{L}_s^{(i)} ds)$ . In this way, I promote  $p_E$  (and  $\tilde{p}_E$ ) to time dependent functions, whose infimum over  $t > 0$  provides the ultimate minimum error probability  $p_E^*$  (and  $\tilde{p}_E^*$ ) for discriminating between the dynamical maps, with (and without) use of side entanglement. I remark that when both dynamical processes are Hamiltonian, i.e.  $\mathcal{L}_t^{(i)} = -i[H_t^{(i)}, \cdot]$ , entanglement never improves discrimination, since the two corresponding channels  $\mathcal{E}_t^{(i)}$  are unitary [12–14].

### 3. The case of two Pauli dynamical maps

In the following I consider the explicit case of two Pauli dynamical maps for qubits, namely

$$\partial_t \rho(t) = \mathcal{L}^{(i)} \rho(t) = \sum_{k=1}^3 \gamma_k^{(i)} [\sigma_k \rho(t) \sigma_k - \rho(t)] . \quad (4)$$

where  $\{\sigma_1, \sigma_2, \sigma_3\} = \{\sigma_x, \sigma_y, \sigma_z\}$  denote the Pauli matrices, and  $\boldsymbol{\gamma}^{(i)} \equiv \{\gamma_x^{(i)}, \gamma_y^{(i)}, \gamma_z^{(i)}\}$  represent the vector of the pertaining decay rates. These maps are purely dissipative, have time-independent generators, and describe two distinct semi-group Markovian dynamics. The solutions  $\mathcal{E}_t^{(i)} = e^{\mathcal{L}^{(i)} t}$  of Eq. (4) define two sets of Pauli channels  $\mathcal{E}_t^{(1)}$  and  $\mathcal{E}_t^{(2)}$ , namely

$$\rho^{(i)}(t) = \mathcal{E}_t^{(i)}(\rho(0)) = \sum_{k=0}^3 p_k^{(i)}(t) \sigma_k \rho(0) \sigma_k , \quad (5)$$

where I introduced  $\sigma_0 \equiv I$  as the  $2 \times 2$  identity matrix along with the two time-dependent probability vectors  $\{p_k^{(i)}(t)\}$ . These probabilities are related to the decay rates  $\{\gamma_k^{(i)}\}$  in Eq. (4) by the relations [34]

$$p_k^{(i)}(t) = \frac{1}{4} \sum_{l=0}^3 H_{kl} A_l^{(i)}(t) , \quad (6)$$

where  $A_l^{(i)}(t)$  are the components of the vectors

$$A^{(i)}(t) = \begin{pmatrix} 1 \\ e^{-2(\gamma_2^{(i)} + \gamma_3^{(i)})t} \\ e^{-2(\gamma_1^{(i)} + \gamma_3^{(i)})t} \\ e^{-2(\gamma_1^{(i)} + \gamma_2^{(i)})t} \end{pmatrix} , \quad (7)$$

and  $H_{kl}$  denote the elements of the Hadamard matrix

$$H = \begin{pmatrix} 1 & 1 & 1 & 1 \\ 1 & 1 & -1 & -1 \\ 1 & -1 & 1 & -1 \\ 1 & -1 & -1 & 1 \end{pmatrix} . \quad (8)$$

I now recall from Refs. [15, 24] the expressions for the error probabilities (2) and (3) in the case of two Pauli channels  $\mathcal{E}^{(i)}(\rho) = \sum_{k=0}^3 p_k^{(i)} \sigma_k \rho \sigma_k$ . By defining

$$r_k \equiv q_1 p_k^{(1)} - q_2 p_k^{(2)}, \quad (9)$$

one has

$$\tilde{p}_E = (1 - M)/2, \quad (10)$$

where

$$M = \max\{|r_0 + r_3| + |r_1 + r_2|, |r_0 + r_1| + |r_2 + r_3|, |r_0 + r_2| + |r_1 + r_3|\}. \quad (11)$$

The three cases compared inside the curly brackets corresponds to feeding the unknown channel with an eigenstate of  $\sigma_z$ ,  $\sigma_x$ , and  $\sigma_y$ , respectively.

On the other hand, the error probability obtained when using side entanglement is given by [15, 24]

$$p_E = (1 - \sum_{k=0}^3 |r_k|)/2, \quad (12)$$

and is achieved by using an arbitrary two-qubit maximally entangled input state. Entanglement strictly improves the discrimination, i.e.  $p_E < \tilde{p}_E$ , iff  $\sum_{k=0}^3 r_k < 0$ .

With these results, I have provided all the necessary ingredients to solve the problem of the optimal discrimination between the two dynamical maps  $\mathcal{L}^{(1)}$  and  $\mathcal{L}^{(2)}$  in Eq. (4), which generate the two possible evolutions of Eq. (5). The error probabilities for discrimination (with and without side entanglement) at time  $t$  can now be evaluated by promoting the values  $r_k$  in Eq. (9) to time-dependent functions, expressed in terms of the time-dependent probabilities  $p_k^{(1)}(t)$  and  $p_k^{(2)}(t)$  obtained by Eq. (6). The resulting time-dependent minimum error probabilities, that henceforth I denote as  $p_E(t)$  and  $\tilde{p}_E(t)$ , can then be further optimised over time  $t$ , yielding the ultimate minimum error probabilities  $p_E^*$  and  $\tilde{p}_E^*$  for distinguishing between the dynamical maps  $\mathcal{L}^{(1)}$  and  $\mathcal{L}^{(2)}$ .

Hereafter, I present explicit solutions for several representative cases. For simplicity, I assume equal prior probabilities, i.e.,  $q_1 = q_2 = \frac{1}{2}$ .

### 3.1. Two dephasing processes along the same direction

Consider two dephasing processes aligned along the same direction, e.g., corresponding to the eigenbasis of  $\sigma_z$ . This implies that in Eq. (4) we take  $\gamma^{(i)} = \{0, 0, \gamma^{(i)}\}$ . The dynamics described by Eq. (5) then corresponds to two dephasing channels with

$$p_0^{(i)}(t) = (1 + e^{-2\gamma^{(i)}t})/2 \quad (13)$$

$$p_1^{(i)}(t) = p_2^{(i)}(t) = 0 \quad (14)$$

$$p_3^{(i)}(t) = (1 - e^{-2\gamma^{(i)}t})/2. \quad (15)$$

Consequently, we obtain

$$p_E(t) = \tilde{p}_E(t) = \frac{1}{2} - \frac{1}{4} \left| e^{-2\gamma^{(1)}t} - e^{-2\gamma^{(2)}t} \right|. \quad (16)$$

Thus, entanglement provides no advantage in discrimination at any time. By solving  $\partial_t p_E(t) = 0$  one finds the optimal time  $t^*$  for comparing the two processes, namely  $t^* = \frac{1}{2(\gamma^{(1)} - \gamma^{(2)})} \ln \frac{\gamma^{(1)}}{\gamma^{(2)}}$ , with the corresponding minimum error probability

$$p_E^* = \tilde{p}_E^* = \frac{1}{2} - \frac{1}{4} \left( \frac{\gamma^{(1)}}{\gamma^{(2)}} \right)^{\frac{\gamma^{(1)}}{\gamma^{(2)} - \gamma^{(1)}}} \left| \frac{\gamma^{(1)}}{\gamma^{(2)}} - 1 \right|. \quad (17)$$

This result shows that  $p_E^*$  depends only on the ratio of the decay rates. Figure 1 illustrates the error probability  $p_E(t)$  for distinguishing a dephasing process with  $\gamma^{(1)} = 1$  from those with  $\gamma^{(2)} = 0.25, 0.5$ , and  $4.0$ .

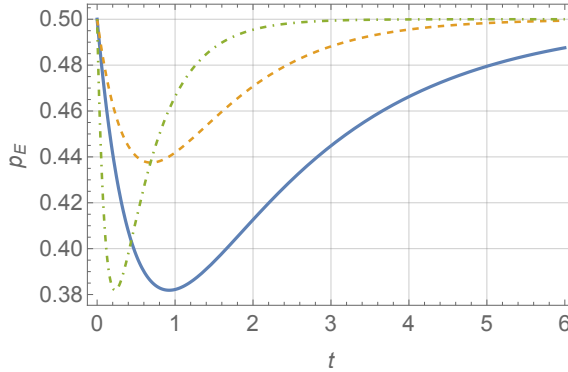


**Figure 1.** Minimum error probability for discriminating at time  $t$  a dephasing process  $\gamma^{(1)} = (0, 0, 1)$  from those with  $\gamma^{(2)} = (0, 0, \gamma^{(2)})$ , where  $\gamma^{(2)} = 0.25, 0.5$ , and  $4.0$  (solid, dashed, and dot-dashed lines, respectively). Entanglement provides no advantage at any time.

### 3.2. Two dephasing processes along orthogonal directions

Now, consider two dephasing processes aligned along orthogonal directions, e.g., corresponding to the mutually unbiased bases of  $\sigma_z$  and  $\sigma_x$ . This means solving the case with  $\gamma^{(1)} = \{0, 0, \gamma^{(1)}\}$  and  $\gamma^{(2)} = \{\gamma^{(2)}, 0, 0\}$ . As before, the dynamics corresponds to dephasing channels, but now the second channel dephases along  $\sigma_x$ , namely

$$p_0^{(2)}(t) = (1 + e^{-2\gamma^{(2)}t})/2 \quad (18)$$

$$p_1^{(2)}(t) = (1 - e^{-2\gamma^{(2)}t})/2 \quad (19)$$

$$p_2^{(2)}(t) = p_3^{(2)}(t) = 0. \quad (20)$$

Thus, we obtain

$$p_E(t) = \tilde{p}_E(t) = \frac{1}{4} \left( 1 + e^{-2 \max\{\gamma^{(1)}, \gamma^{(2)}\} t} \right). \quad (21)$$

Again, entanglement does not enhance discrimination at any time. Clearly, the optimal discrimination occurs at  $t \rightarrow +\infty$ , where  $p_E^* = \tilde{p}_E^* = \frac{1}{4}$ .

### 3.3. Two coplanar decaying processes

Next, consider two processes with  $\gamma^{(i)} = \{\gamma^{(i)}, \gamma^{(i)}, 0\}$ . Each process provides a set of Pauli channels with the time-dependent probabilities

$$p_0^{(i)}(t) = e^{-2\gamma^{(i)}t} \cosh^2(\gamma^{(i)}t) \quad (22)$$

$$p_1^{(i)}(t) = p_2^{(i)}(t) = (1 - e^{-4\gamma^{(i)}t})/4 \quad (23)$$

$$p_3^{(i)}(t) = e^{-2\gamma^{(i)}t} \sinh^2(\gamma^{(i)}t) . \quad (24)$$

In this case, entanglement improves discrimination at any time. Specifically, we have

$$\tilde{p}_E(t) = \frac{1}{2} - \frac{1}{4} \max\{|e^{-2\gamma^{(1)}t} - e^{-2\gamma^{(2)}t}|, |e^{-4\gamma^{(1)}t} - e^{-4\gamma^{(2)}t}|\} , \quad (25)$$

while

$$p_E(t) = \frac{1}{2} - \frac{1}{4}|e^{-2\gamma^{(1)}t} - e^{-2\gamma^{(2)}t}| - \frac{1}{8}|e^{-4\gamma^{(1)}t} - e^{-4\gamma^{(2)}t}| , \quad (26)$$

and, clearly,  $p_E(t) < \tilde{p}_E(t)$ . In the absence of side entanglement, since  $\tilde{p}_E(t)$  has two absolute minima, there are two optimal times given by  $t^* = \frac{\kappa}{\gamma^{(1)} - \gamma^{(2)}} \ln \frac{\gamma^{(1)}}{\gamma^{(2)}}$ , with  $\kappa = 1/2$  or  $1/4$ . At both times, we have

$$\tilde{p}_E^* = \frac{1}{2} - \frac{1}{4} \left( \frac{\gamma^{(1)}}{\gamma^{(2)}} \right)^{\frac{\gamma^{(1)}}{\gamma^{(2)} - \gamma^{(1)}}} \left| \frac{\gamma^{(1)}}{\gamma^{(2)}} - 1 \right| . \quad (27)$$

On the other hand, when using entanglement, there is a unique optimal time  $t^*$  such that  $\partial_t p_E(t) = 0$ , which corresponds to the solution of the transcendental equation

$$\gamma^{(1)}(e^{-4\gamma^{(1)}t} + e^{-2\gamma^{(1)}t}) = \gamma^{(2)}(e^{-4\gamma^{(2)}t} + e^{-2\gamma^{(2)}t}) . \quad (28)$$

Figure 2 shows the error probabilities from Eqs. (25) and (26) for  $\gamma^{(1)} = 1$  and  $\gamma^{(2)} = 0.2$ . The ultimate minimum error probability,  $p_E^* \simeq 0.308$ , is achieved using entanglement, with discrimination performed at the optimal time  $t^* \simeq 0.782$ .

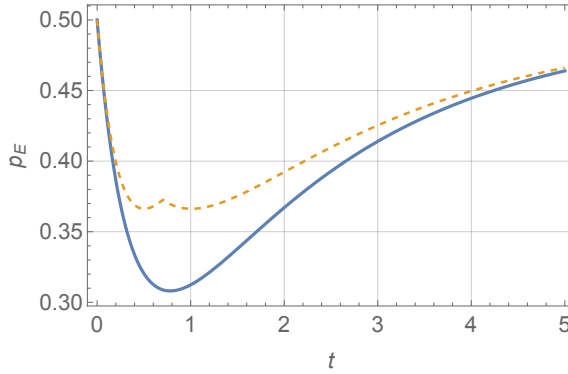


**Figure 2.** Minimum error probabilities for discriminating between two coplanar decaying processes with  $\gamma^{(1)} = (1, 1, 0)$  and  $\gamma^{(2)} = (.2, .2, 0)$  at time  $t$ , with and without entanglement (solid and dashed lines, respectively). Side entanglement strictly improves discrimination at any time.

### 3.4. Two depolarising processes

In a depolarising process, the decay rates have equal and constant components. Thus, we consider the case with  $\gamma^{(i)} = \{\gamma^{(1)}, \gamma^{(2)}, \gamma^{(3)}\}$ . The dynamics of each process gives a set depolarising channels with the time-dependent probabilities

$$p_0^{(i)}(t) = (1 + 3e^{-4\gamma^{(i)}t})/4 \quad (29)$$

$$p_1^{(i)}(t) = p_2^{(i)}(t) = p_3^{(i)}(t) = (1 - e^{-4\gamma^{(i)}t})/4. \quad (30)$$

Thus, we obtain

$$\tilde{p}_E(t) = \frac{1}{2} - \frac{1}{4}|e^{-4\gamma^{(1)}t} - e^{-4\gamma^{(2)}t}|, \quad (31)$$

$$p_E(t) = \frac{1}{2} - \frac{3}{8}|e^{-4\gamma^{(1)}t} - e^{-4\gamma^{(2)}t}|. \quad (32)$$

Clearly, entanglement enhances discrimination at any time. Figure 3 illustrates this for the specific values  $\gamma^{(1)} = 1$  and  $\gamma^{(2)} = 0.2$ .

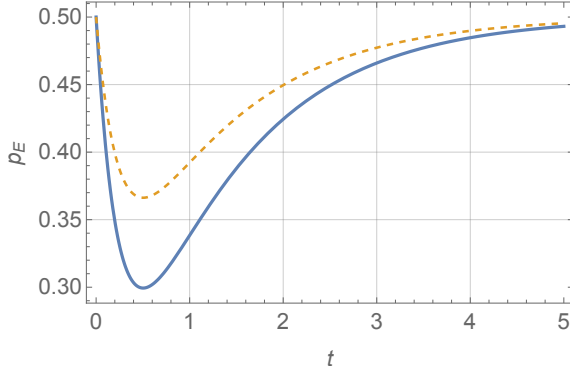


**Figure 3.** Minimum error probability for discriminating two depolarising processes at time  $t$ , with  $\gamma^{(1)} = (1, 1, 1)$  and  $\gamma^{(2)} = (0.2, 0.2, 0.2)$ , with and without entanglement assistance (solid and dashed lines, respectively).

Notice that both  $\tilde{p}_E(t)$  and  $p_E(t)$  reach their minimum at the same optimal time

$$t^* = \frac{1}{4(\gamma^{(1)} - \gamma^{(2)})} \ln \frac{\gamma^{(1)}}{\gamma^{(2)}}, \quad (33)$$

with the corresponding ultimate minimum error probabilities given by

$$\tilde{p}_E^* = \frac{1}{2} - \frac{1}{4} \left( \frac{\gamma^{(1)}}{\gamma^{(2)}} \right)^{\frac{\gamma^{(1)}}{\gamma^{(2)} - \gamma^{(1)}}} \left| \frac{\gamma^{(1)}}{\gamma^{(2)}} - 1 \right|, \quad (34)$$

$$p_E^* = \frac{1}{2} - \frac{3}{8} \left( \frac{\gamma^{(1)}}{\gamma^{(2)}} \right)^{\frac{\gamma^{(1)}}{\gamma^{(2)} - \gamma^{(1)}}} \left| \frac{\gamma^{(1)}}{\gamma^{(2)}} - 1 \right|. \quad (35)$$

These error probabilities are shown in Fig. 4 as a function of the ratio of the decay parameters  $\gamma^{(1)}$  and  $\gamma^{(2)}$ .

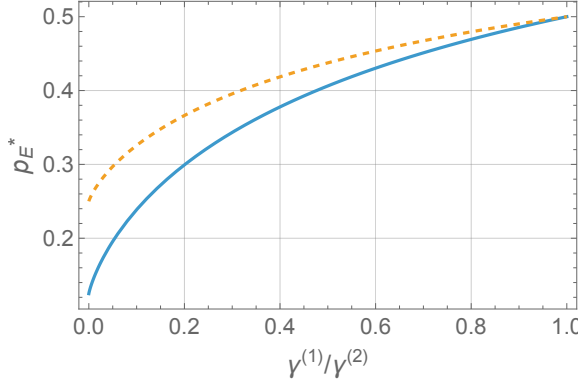


**Figure 4.** Ultimate minimum error probabilities in discriminating between two depolarising processes as a function of the ratio of the decay rates, with and without entanglement assistance (solid and dashed lines, respectively). In both cases, the optimal discrimination time is given by Eq. (33).

### 3.5. A depolarising and a dephasing process

Finally, let us consider the problem of distinguishing between a depolarising process,  $\gamma^{(1)} = \{\gamma^{(1)}, \gamma^{(1)}, \gamma^{(1)}\}$ , and a dephasing process,  $\gamma^{(2)} = \{0, 0, \gamma^{(2)}\}$ . For a strategy with no use of entanglement the error probability is given by

$$\tilde{p}_E(t) = \frac{1}{2} - \frac{1}{4} \max\{1 - e^{-4\gamma^{(1)}t}, |e^{-4\gamma^{(1)}t} - e^{-2\gamma^{(2)}t}|\}. \quad (36)$$

In this case, the infimum is achieved in the limit  $t \rightarrow +\infty$ , where  $\tilde{p}_E^* = \frac{1}{4}$ .

By utilizing entanglement, the error probability is instead given by

$$\begin{aligned} p_E(t) = & \frac{1}{2} - \frac{1}{8}(1 - e^{-4\gamma^{(1)}t}) - \frac{1}{16}|1 - 3e^{-4\gamma^{(1)}t} + 2e^{-2\gamma^{(2)}t}| \\ & - \frac{1}{16}|1 + e^{-4\gamma^{(1)}t} - 2e^{-2\gamma^{(2)}t}|. \end{aligned} \quad (37)$$

The comparison between these two strategies is more intricate than in previous cases. By analyzing the two functions (36) and (37), we find that they are equal  $p_E(t) = \tilde{p}_E(t) = \frac{1}{4}(1 + e^{-4\gamma^{(1)}t})$  at all times when

$$3e^{-4\gamma^{(1)}t} - 1 \leq 2e^{-2\gamma^{(2)}t} \leq e^{-4\gamma^{(1)}t} + 1. \quad (38)$$

To determine whether entanglement provides a strict advantage, we must identify a time  $t^*$  at which  $p_E(t)$  reaches a minimum value lower than  $\frac{1}{4}$ . Notice that the condition  $p_E(t) \leq \frac{1}{4}$  can be satisfied in the region

$$e^{-2\gamma^{(2)}t} \geq (3e^{-4\gamma^{(1)}t} + 1)/2, \quad (39)$$

where

$$p_E(t) = (3 + 3e^{-4\gamma^{(1)}t} - 2e^{-2\gamma^{(2)}t})/8. \quad (40)$$

In fact, numerical inspection shows that this condition holds as long as  $\frac{\gamma^{(2)}}{\gamma^{(1)}} \lesssim 0.3785$ .

In this case the minimum of  $p_E(t)$  in Eq. (40) is reached at  $t^* = \frac{1}{4\gamma^{(1)} - 2\gamma^{(2)}} \ln \frac{3\gamma^{(1)}}{\gamma^{(2)}}$ , with

a corresponding minimum error probability

$$p_E^* = \frac{3}{8} \left[ 1 - \left( \frac{3\gamma^{(1)}}{\gamma^{(2)}} \right)^{\frac{2\gamma^{(1)}}{\gamma^{(2)} - 2\gamma^{(1)}}} \left( \frac{2\gamma^{(1)}}{\gamma^{(2)}} - 1 \right) \right] < \frac{1}{4}. \quad (41)$$

Thus, when  $\frac{\gamma^{(2)}}{\gamma^{(1)}} \lesssim 0.3785$ , entanglement provides a strict advantage in discrimination at a finite time. Figure 5 illustrates this threshold, where the benefits of entanglement are clearly visible.

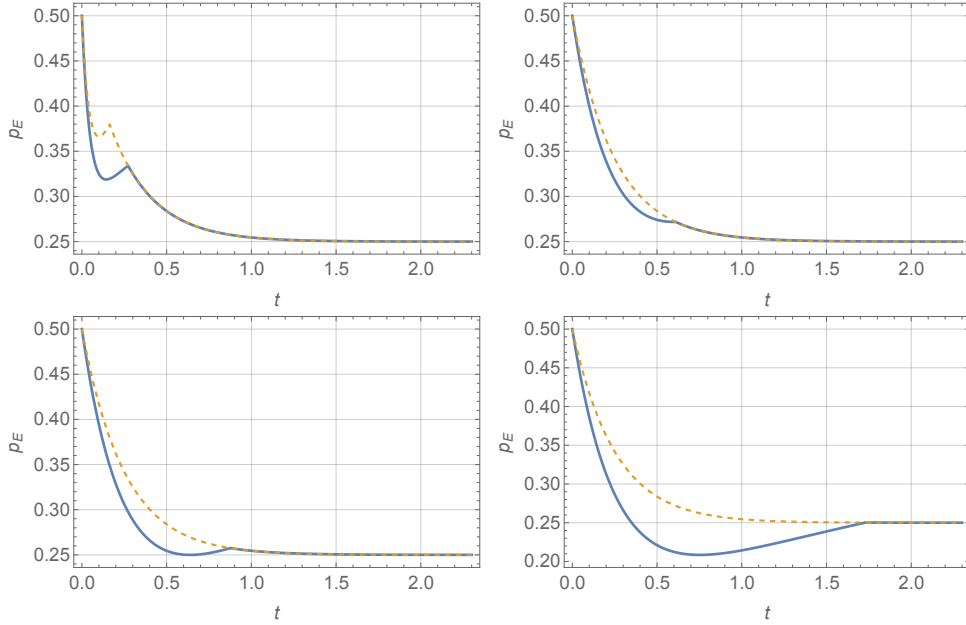


**Figure 5.** Minimum error probability for discriminating the depolarising process  $\gamma^{(1)} = (1, 1, 1)$  from a dephasing process  $\gamma^{(2)} = (0, 0, \gamma^{(2)})$  with and without side entanglement (solid and dashed lines, respectively), for different values of  $\gamma^{(2)}$ : 10 (top left), 0.5 (top right), 0.3785 (bottom left), and 0.2 (bottom right).

#### 4. Conclusions

This work deepens our understanding of the discrimination of quantum dynamical processes by uncovering the crucial interplay between entanglement, timing, and optimal measurement strategies. By showing that entangled input states can enable optimal discrimination at finite times—whereas separable strategies may require waiting indefinitely until stationarity—this study highlights the operational value of quantum correlations in time-sensitive tasks. These results establish a concrete foundation for designing more efficient discrimination protocols and underscore the broader utility of entanglement in dynamically evolving quantum systems.

The findings naturally invite several directions for future research, including extensions to more complex dynamical scenarios such as processes governed by

inequivalent Lindbladian generators or exhibiting non-Markovian features. From a practical perspective, the results have direct relevance to quantum metrology, error correction, and sensing, where rapid and reliable identification of dynamical behavior is often critical. In particular, in applications like quantum illumination, optimal timing may correspond to optimal spatial configurations—such as the distance to a target—further illustrating the practical implications of temporal optimisation in real-world quantum technologies.

## Acknowledgments

This work has been sponsored by PRIN MUR Project 2022SW3RPY.

## References

- [1] C. W. Helstrom, *Quantum Detection and Estimation Theory* (Academic Press, New York, 1976).
- [2] I. D. Ivanovic, Phys. Lett. A **123**, 257 (1987).
- [3] D. Dieks, Phys. Lett. A **126**, 303 (1988).
- [4] A. Peres, Phys. Lett. A **128**, 19 (1988).
- [5] G. Jaeger and A. Shimony, Phys. Lett. A **197**, 83 (1995).
- [6] J. Walgate, A. J. Short, L. Hardy, and V. Vedral, Phys. Rev. Lett. **85**, 4972 (2000).
- [7] S. Virmani, M. F. Sacchi, M. B. Plenio, and D. Markham, Phys. Lett. A **288**, 62 (2001).
- [8] J. Bergou, U. Herzog, and M. Hillery, *Quantum state estimation*, Lecture Notes in Physics Vol. 649 (Springer, Berlin, 2004), p. 417; A.Chefles, *ibid.*, p. 467.
- [9] G. M. D'Ariano, M. F. Sacchi, and J. Kahn, Phys. Rev. A **72**, 032310 (2005).
- [10] F. Buscemi and M. F. Sacchi, Phys. Rev. A **74**, 052320 (2006).
- [11] J. Bae and L.-C. Kwek, J. Phys. A **48**, 083001 (2015).
- [12] A. M. Childs, J. Preskill, and J. Renes, J. Mod. Opt. **47**, 155 (2000).
- [13] A. Acín, Phys. Rev. Lett. **87**, 177901 (2001).
- [14] G. M. D'Ariano, P. Lo Presti, and M. G. A. Paris, Phys. Rev. Lett. **87**, 270404 (2001).
- [15] M. F. Sacchi, Phys. Rev. A **71**, 062340 (2005).
- [16] M. F. Sacchi, Phys. Rev. A **72**, 014305 (2005).
- [17] G. Chiribella, G. M. D'Ariano, and P. Perinotti, Phys. Rev. Lett. **101**, 180501 (2008).
- [18] K. Nakahira and K. Kato, Phys. Rev. Lett. **126**, 200502 (2021).
- [19] S. K. Oskouei, S. Mancini, and M. Rexiti, Proc. R. Soc. A **479**, 20220796 (2023).
- [20] S. Lloyd, Science **321**, 1463 (2008).
- [21] S.-H. Tan, B. I. Erkmen, V. Giovannetti, S. Guha, S. Lloyd, L. Maccone, S. Pirandola, and J. H. Shapiro, Phys. Rev. Lett. **101**, 253601 (2008).
- [22] M. Sanz, U. Las Heras, J. J. García-Ripoll, E. Solano, and R. Di Candia, Phys. Rev. Lett. **118**, 070803 (2017).
- [23] J. H. Shapiro, IEEE Aerospace and Electronic Systems Magazine **35**, 8 (2020).
- [24] M. F. Sacchi, J. Opt. B **7**, S333 (2005).
- [25] G. M. D'Ariano, M. F. Sacchi, and J. Kahn, Phys. Rev. A **72**, 052302 (2005).
- [26] S. Jevtic, D. Newman, T. Rudolph, and T. M. Stace, Phys. Rev. A **91**, 012331 (2015).
- [27] A. Candeloro and M. G. A. Paris, Phys. Rev. A **103**, 012217 (2021).
- [28] D. Farina, V. Cavina, and V. Giovannetti, Phys. Rev. A **100**, 042327 (2019).
- [29] D. Farina, V. Cavina, M. G. Genoni, and V. Giovannetti, Phys. Rev. A **106**, 042609 (2022).
- [30] H.-P. Breuer and F. Petruccione, *The theory of open quantum systems* (Oxford University Press, Oxford, 2002).
- [31] A. Rivas and S. F. Huelga, *Open quantum systems*, Vol. 10 (Springer, Berlin/Heidelberg, 2012).

- [32] V. I. Paulsen, *Completely Bounded Maps and Dilations* (Longman Scientific and Technical, New York, 1986).
- [33] D. Aharonov, A. Kitaev, and N. Nisan, in “Proceedings of the 30th Annual ACM Symposium on Theory of Computation (STOC)”, p. 20, 1997.
- [34] D. Chruściński and F. A. Wudarski, Phys. Lett. A **377**, 1425 (2013).